IEEE Photonics Journal
An IEEE Photonics Society Publication

Open Access

Polarization-Insensitive Remote Access Unit for Radio-Over-Fiber Mobile Fronthaul System by Reusing Polarization Orthogonal Light Waves

Volume 8, Number 1, February 2016

Beilei Wu
Jiun-Yu Sung
Jhih-Heng Yan
Mu Xu
Jing Wang
Fengping Yan
Shuisheng Jian
Gee-Kung Chang, Fellow, IEEE

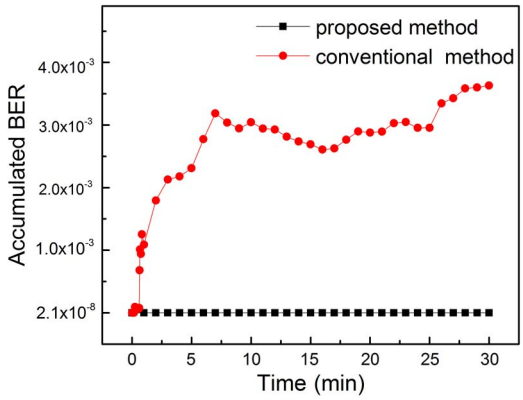

DOI: 10.1109/JPHOT.2015.2508426
1943-0655

IEEE photonics SOCIETY

IEEE

Polarization-Insensitive Remote Access Unit for Radio-Over-Fiber Mobile Fronthaul System by Reusing Polarization Orthogonal Light Waves

Beilei Wu,[1,2] Jiun-Yu Sung,[2,3] Jhih-Heng Yan,[2,4] Mu Xu,[2] Jing Wang,[2] Fengping Yan,[1] Shuisheng Jian,[1] and Gee-Kung Chang,[2] *Fellow, IEEE*

[1]Institute of Lightwave Technology, Key Lab of All Optical Network and Advanced Telecommunication of EMC, Beijing Jiaotong University, Beijing 100044, China
[2]School of Electrical and Computer Engineering, Georgia Institute of Technology, Atlanta, GA 30332 USA
[3]Department of Photonics and Institute of Electro-Optical Engineering, National Chiao Tung University, Hsinchu 30010, Taiwan
[4]Institute of Photonics Technologies, National Tsing Hua University, Hsinchu 30013, Taiwan

DOI: 10.1109/JPHOT.2015.2508426

Manuscript received November 17, 2015; revised December 6, 2015; accepted December 8, 2015. Date of publication December 17, 2015; date of current version January 29, 2016. This work was supported in part by the Georgia Institute of Technology and in part by the National Natural Science Foundation of China under Grant 61275091 and Grant 61327006. The work of B. Wu was supported by the China Scholarship Council. Corresponding author: F. Yan (e-mail: fpyan@bjtu.edu.cn).

Abstract: To reduce the complexity and cost of remote access units (RAUs), colorless transport architecture is preferred in a wavelength-division multiplexing (WDM) system. The wavelength-reuse technique is commonly adopted to realize colorless RAUs. However, in traditional approaches, RAUs employ crystal-based Mach–Zehnder modulators (MZMs) to modulate the distributed carriers. Hence, polarization tracking systems are necessary to align the polarization state of the distributed carriers with the MZM principal axis. This increases the cost of the RAUs. In this paper, a full-duplex millimeter-wave (MMW) radio-over-fiber (RoF) access architecture employing polarization-insensitive RAUs is proposed. In our proposed RAUs, the upstream signals are generated using polarization-orthogonal lights, and the performance of the upstream signals is independent of the polarization state of the MZM input lights. The proposed system is mathematically formulated and experimentally demonstrated. The 1.2-Gb/s quadrature phase-shift keying (QPSK) orthogonal frequency-division multiplexing (OFDM) downstream signal at the 60-GHz band and 5-Gb/s on–off keying (OOK) polarization-insensitive upstream signal over a 15-km standard single-mode fiber (SSMF) are demonstrated. In our results, a polarization-insensitive RAU is successfully obtained. The power penalty resulting from the interference of downstream signal is about 0.4 and 0.6 dB with a bit error rate (BER) of 10^{-9} in back-to-back and 15-km fiber transmission, respectively.

Index Terms: Radio-over-fiber (RoF), remote access units, polarization-insensitive.

1. Introduction

In view of massive proliferation of smart mobile devices, system capacity requirement for wireless applications is rapidly increasing. Optical fiber for mobile fronthaul is widely recognized as the future-proof solution in order to maintain the coverage of a central station (CS), with links

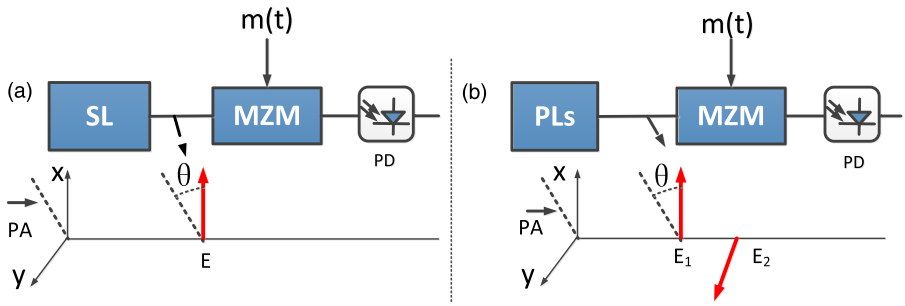

Fig. 1. Schematic diagrams of (a) the conventional modulation scheme and (b) the proposed polarization-insensitive modulation scheme. SL: single-wavelength light; PLs: polarization-orthogonal lights; PA: principal axis.

between the CS and the remote access units (RAUs). To solve the current spectrum crunch for the frequency bands, wireless transmission using millimeter wave (MMW) is extensively investigated [1]–[3]. Besides, radio-over-fiber (RoF) architecture is also widely investigated to further reduce the complexity and cost of the RAUs [4]–[7].

Data distributed from a CS to the RAUs are commonly provided using wavelength-division multiplexing (WDM) technique. The transmission wavelengths used by a specific RAU should be accurately controlled. In order to reduce the maintenance cost of RAUs, colorless RAUs are preferable. A colorless RAU can be easily achieved using wavelength-reuse techniques [8]–[13]. While wavelength-reuse techniques are adopted, the optical carriers used for upstream transmission are distributed from the CS and modulated by other devices installed in the RAUs. Mach–Zehnder modulators (MZMs) using $LiNbO_3$ are commonly used in the RAUs to modulate the distributed carriers. However, some polarization manipulation approaches should be used to align the distributed carriers with the principal axis (PA) of the $LiNbO_3$ crystal in the MZM. The complexity and cost of RAUs will thus increase. Electro-absorption modulator (EAM) was proposed for polarization-insensitive modulation [14]. However, due to its possible chirp issues, it is still questionable if EAM will be an ultimate choice [15].

In this paper, a bidirectional MMW-RoF mobile fronthaul architecture with colorless and polarization-insensitive RAUs is proposed. In the CS, an optical signal composed of two polarization-orthogonal un-modulated optical tones and one modulated signal is generated. In the RAU, the MMW is generated by coherent beating between the modulated signal and the unmodulated carrier. The unmodulated polarization-orthogonal optical tones are further used to carry the upstream data through a crystal based MZM. Since the overall power aligned on the PA of the $LiNbO_3$ crystal in the MZM is an invariant, the modulation depth of the output signal is independent to the relative polarization states of the input lights. The polarization-independent feature of the proposed scheme is analyzed mathematically and proved experimentally. 1.2 Gb/s quadrature-phase-shift-keying (QPSK) orthogonal frequency-division multiplexing (OFDM) downstream signals (DS) at 60 GHz band and 5 Gb/s on-off keying (OOK) polarization-insensitive upstream signal (US) over 15 km standard single-mode fiber (SSMF) are demonstrated. Performance comparisons between the proposed scheme and the conventional scheme (using single-wavelength light (SL) for the upstream modulation) are also provided.

2. Operation Principles

Fig. 1(a) is the architecture of the conventional wavelength-reuse scheme (using SL for modulation). In the RAU, the polarization state of the input carrier is tracked and aligned with the PA of the MZM crystal (shown as the dashed line in Fig. 1). While the polarization state of the input light and the PA of the MZM crystal are not well aligned, the modulation depth will decrease and degrade the signal performance. Recently, automatic polarization trackers have been proposed and demonstrated in practical systems [16]–[19]. The adaptive loop-based polarization tracking

system may be used to align the polarization state of the signal with the MZM modulation axis. However, this results in additional system complexity and cost. Hence, polarization-independent modulation schemes may be more preferable.

Fig. 1(b) is our proposed scheme. The US is modulated on the polarization-orthogonal lights (PLs), which we name them E_1 and E_2 respectively. By adequately controlling the relative power of E_1 and E_2, they can have identical amplitude E_0. While we define the polarization direction of E_1 as the coordinate x-axis as shown in Fig. 1(b), the fields of E_1 and E_2 can be represented as

$$E_1 = \begin{bmatrix} E_0 \cdot e^{j\omega_1 t+\varphi_1} \\ 0 \end{bmatrix}, \quad E_2 = \begin{bmatrix} 0 \\ E_0 \cdot e^{j\omega_2 t+\varphi_2} \end{bmatrix} \tag{1}$$

where ω_1 and ω_2 are, respectively, the center frequencies of E_1 and E_2, and φ_1 and φ_2 are their initial phase constants. To avoid confusion, the nonlinear behavior of the MZM is not considered here. The MZM is modeled as an ideal modulator which transforms the electrical signal into the optical field without any distortion. If we assume the PA of the MZM crystal is aligned to the x-axis with an arbitrarily angle θ, the Jones matrix of the MZM can be expressed as

$$\begin{aligned} Q &= \begin{bmatrix} \cos(\theta) & -\sin(\theta) \\ \sin(\theta) & \cos(\theta) \end{bmatrix} \begin{bmatrix} m(t) & 0 \\ 0 & 1 \end{bmatrix} \begin{bmatrix} \cos(\theta) & \sin(\theta) \\ -\sin(\theta) & \cos(\theta) \end{bmatrix} \\ &= \frac{1}{2} \begin{bmatrix} (m-1)\cos(2\theta)+m+1 & (m-1)\sin(2\theta) \\ (m-1)\sin(2\theta) & (m+1)-(m-1)\cos(2\theta) \end{bmatrix} \end{aligned} \tag{2}$$

where $m = m(t)$ is the modulation signal. After the modulation process, the received photocurrent after the photo-diode (PD) is

$$\begin{aligned} i_{PD} &\propto |QE_1|^2 + |QE_2|^2 \\ &= \frac{E_0^2}{4} \left\{ [(m-1)\cos(2\theta)+m+1]^2 + 2[(m-1)\sin(2\theta)]^2 + [(m+1)-(m-1)\cos(2\theta)]^2 \right\} \\ &= E_0^2(m^2+1). \end{aligned} \tag{3}$$

The cross-beating terms between E_1 and E_2 do not appear since E_1 and E_2 are orthogonally polarized. From (3), we can see that the generated photocurrent is independent to the value of θ. Hence, it is not necessary to align the polarization state of the optical signal with the PA of the MZM crystal in the RAU. The RAU is polarization insensitive.

3. Experiment Setup and Results

Fig. 2 illustrates the experimental setup of the proposed architecture. A single-wavelength optical carrier was output from a laser diode (LD). The center wavelength of the optical carrier was 1553.69 nm. The optical carrier was split into two branches by a 50/50 optical coupler. In the upper branch, the optical carrier was modulated by a 20 GHz local oscillator (LO1) through MZM1. MZM1 was biased at its null point to suppress the zero-order carrier. Thus, two optical tones with 40 GHz frequency spaces generated after MZM1. Inset (a) of Fig. 2 was the conceptual spectrum of the optical two tones. The optical two tones were then input into MZM2 which was biased at its quadrature point. MZM2 was driven by an intermediate frequency (IF) signal. The IF signal was generated by mixing the 1.2 Gb/s QPSK-OFDM signal with a 20 GHz sine-wave source (generated by LO2). The QPSK-OFDM signal was generated by an arbitrary waveform generator (AWG) with 12 GSa/s sampling rate. The conceptual spectrum of the output signal from MZM2 was shown in inset (c) of Fig. 2. After MZM2, a 33/66 optical interleaver (IL) was used to filter the trivial wavelengths. The optical single-sideband (OSSB) RoF signal was generated after the IL as depicted in inset (d) of Fig. 2. The experimentally measured optical spectra before and after the IL were respectively shown in Fig. 3(a) and (b). The RoF signal was combined with the un-modulated optical carrier in the lower branch through a polarization beam combiner (PBC). The PLs were obtained after the PBC as shown in inset (e) of Fig. 2. A

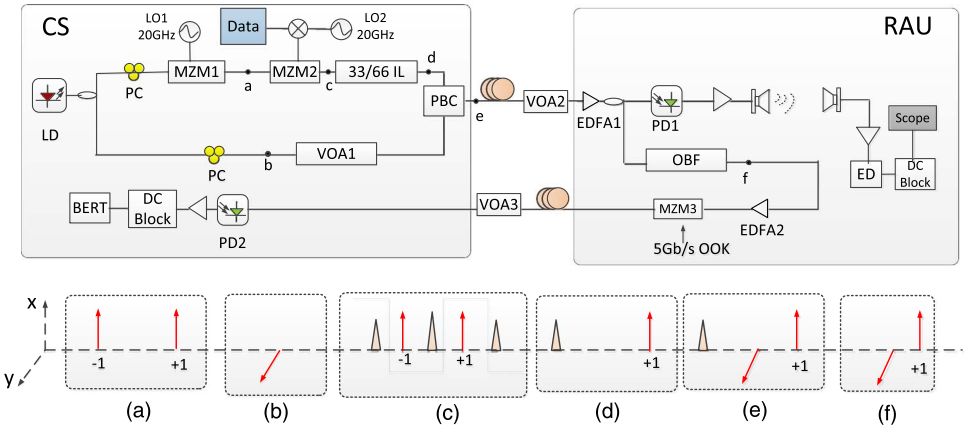

Fig. 2. Experimental setup of the proposed architecture. (Insets) (a)–(f) Conceptual optical spectra at location a–f. LD: laser diode; LO: local oscillator; CS: central station; RAU: remote access unit; PC: polarization controller; PD: photo-diode; IL: interleaver; PBC: polarization beam combiner; OBF: optical band-pass filter; ED: envelope detector; VOA: variable optical attenuator; DC: direct current.

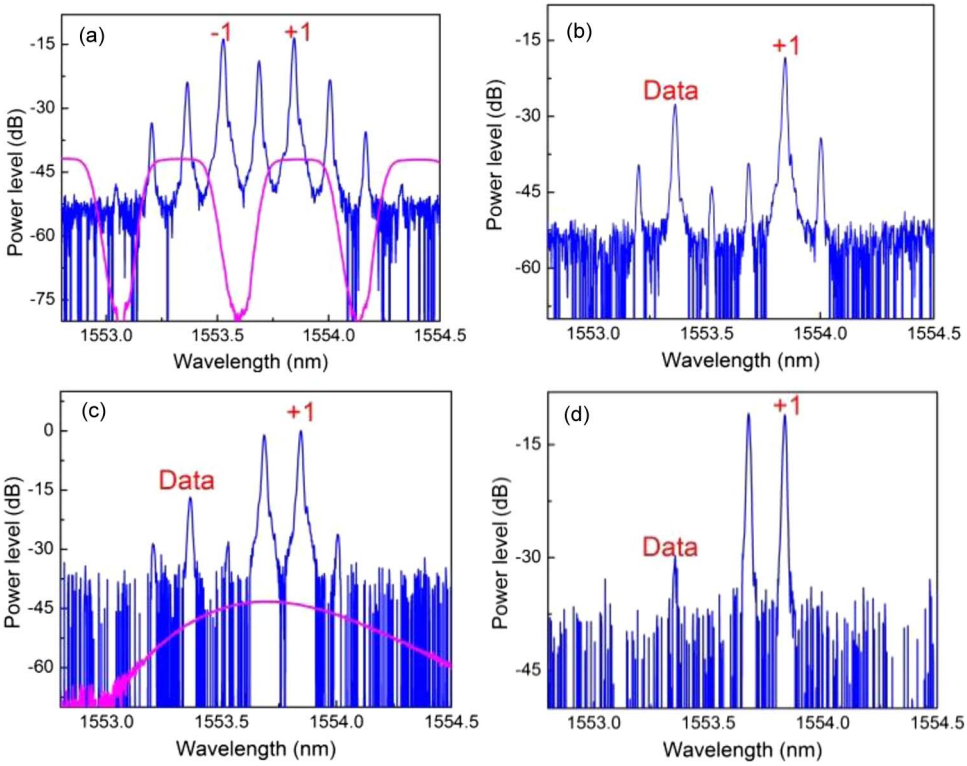

Fig. 3. Optical spectra measured at different positions of Fig. 2. (a) Output of MZM2 (blue line) and the 33/66 IL transmission response (purple line). (b) Output of the 33/66 IL. (c) Input of the OBF (blue line) and the OBF transmission response (purple line). (d) Output of the OBF.

polarization controller (PC) and a variable optical attenuator (VOA) were used in the lower branch to make sure the power of the two orthogonal tones (carrier and +1st sideband) was equal. After the PBC, the resultant optical signal was transmitted over a 15 km SSMF to the RAU.

At the RAU, the optical signal was divided into two signals by an optical coupler. The first signal was received by a high speed PD (PD1). An erbium-doped fiber amplifier (EDFA) was used in front of PD1 to compensate the power loss in the CS and the fiber. The desired MMW signal

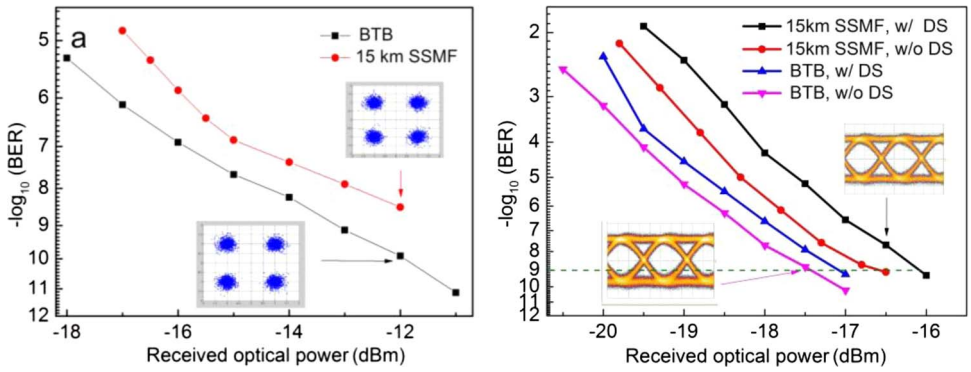

Fig. 4. Signal performance. (a) BER versus received optical power for the DS. (b) BER versus received optical power for the US.

was obtained after PD1. A pair of 60-GHz horn antennas with 2-ft separation was used for wireless communication. After the receiving antenna, an envelope detector (ED) was used to retrieve the envelope of the signal. The envelope of the signal was recorded by a real-time oscilloscope with 40 GSa/s sampling rate and the QPSK-OFDM signal was decoded offline. At the other output port of the optical coupler, the polarization-orthogonal unmodulated tones were selected by the optical band-pass filter (OBF) as illustrated in inset (f) of Fig. 2. The experimentally measured optical spectra before and after the OBF were respectively shown in Fig. 3(c) and (d). Another EDFA (EDFA2) was used to increase the input power to MZM3 to maintain the optical signal-to-noise ratio (OSNR) of the signal. Then, as discussed in Section 2, the resultant PLs were input into MZM3. The PLs were modulated by the 5 Gb/s OOK signal through MZM3. Then another 15 km SSMF was used to transmit the US. In the CS, the US was received by PD2 and analyzed by a bit error rate (BER) tester. Here the downstream data rate is lower than that of the upstream signal due to the bandwidth limitation of our wireless components. In order to show the high speed capability of our system, we are not decreasing our upstream data rate to make it lower than the downstream signal, which is the conventional case. Since we can achieve higher data rate without the wireless transmission, it is believed that our downstream data rate may increase while devices with wider bandwidth are used.

To characterize the signal quality, the error vector magnitude (EVM) of DS is calculated according to our decoded signal. Then the signal BER is estimated from the EVM according to the equation provided by [20]. Fig. 4(a) shows the BER performance of the DS versus the RAU receiving optical power. The insets are respectively the resultant constellations for back-to-back (BTB) and 15 km fiber transmission cases while the RAU receiving power is −12 dBm. We can observe that signal performance with BER about 10^{-9} can be roughly obtained; hence forward error correction (FEC) is not necessary. This decreases the RAU system complexity. Fig. 4(b) shows the BER performance of the upstream OOK signal while the DS is, respectively, transmitted or closed at both BTB and 15 km fiber transmission. BER lower than 10^{-9} can be obtained for the US. A power penalty of 0.4 dB and 0.6 dB at BER $= 10^{-9}$ can be observed while the DS is transmitted simultaneously in BTB and 15 km fiber transmission, respectively. This may come from the additional interference, as shown in Fig. 3(d) (the DS is not completely filtered). About 0.8 dB and 1 dB power penalty at BER $= 10^{-9}$ are shown due to fiber transmission for without DS and with DS case, respectively. Insets of Fig. 4(b) are the clear eye diagrams for the BTB case and 15 km fiber transmission.

The polarization sensitivity of the conventional (using SL) and the proposed (using PLs) schemes for the upstream transmission is studied. In the experiment setup for the conventional scheme, the lower branch of the CS in Fig. 2 was removed. Hence the optical spectrum of the signal transmitted to the RAU is similar with the spectrum in Fig. 3(b). In the RAU, after the OBF, only SL (+1st sideband) was reused for the upstream transmission. For both the

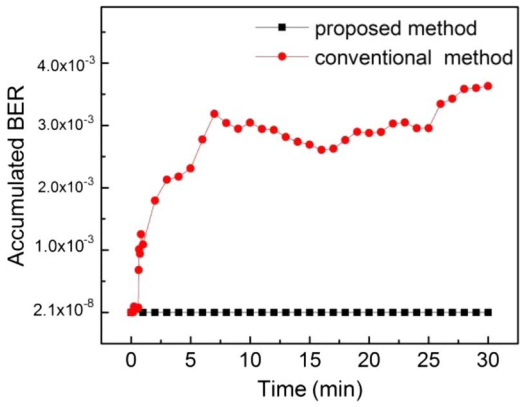

Fig. 5. Comparison of the accumulated BER time trace between the conventional modulation scheme and the proposed polarization-insensitive scheme.

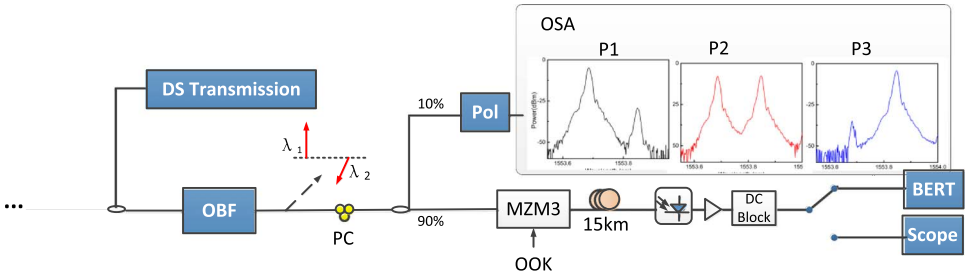

Fig. 6. Experimental setup for comparing the performance difference among different schemes. (Inset) Optical spectra to determine the relative polarization states of the PLs for the proposed wavelength reusing scheme. OBF: optical band-pass filter; PC: polarization controller; Pol: polarizer; OSA: optical spectrum analyzer. BERT: bit error rate tester.

conventional and our proposed upstream schemes, a polarization scrambler was used before MZM3. Fig. 5 shows the resultant BER time trace for different schemes at BTB transmission. For the conventional scheme, the BER value fluctuates and quickly accumulates to the order of 10^{-3}. Since the scenario that the polarization state of the input light is orthogonal with the PA of MZM crystal occurs frequently, the overall BER will never recover back to the order of 10^{-9}. Compared to the conventional scheme, our proposed scheme has better BER performance with a more flat time trace.

Another experiment was further performed to analyze how different polarization states will contribute to the overall signal performance. The experiment setup of the CS is identical to Fig. 2. A modified setup was set in the RAU as shown in Fig. 6. A PC and a 90/10 optical coupler were further used before MZM3 in the RAU. For our proposed scheme, the PLs were selected by the OBF [see Fig. 2(f)] and were divided into two streams by a 90/10 coupler after a PC. The PC was used to change the polarization state of the light waves. The 10% PLs were input into a polarizer (Pol) and monitored by an optical spectrum analyzer (OSA). The relative polarization states of the PLs are estimated according to the optical spectrum after the Pol. Three arbitrary polarization states (P1, P2 and P3) were chosen whose optical spectra were shown as insets of Fig. 6. For the conventional scheme, the PC was also used before MZM3 to change the polarization state of the input light wave. Three polarization states were chosen according to the measured eye diagrams (see the insets of Fig. 7): (1) parallel to the PA of MZM3 crystal (P4), (2) deviated from the PA of MZM3 crystal (P5), and (3) completely orthogonal to the PA of MZM3 crystal (P6). The resultant BER performance for different schemes is shown in Fig. 7. For the conventional scheme, only P4 can reach BER 10^{-9} level. While the FEC threshold of BER 3.8×10^{-3} is considered,

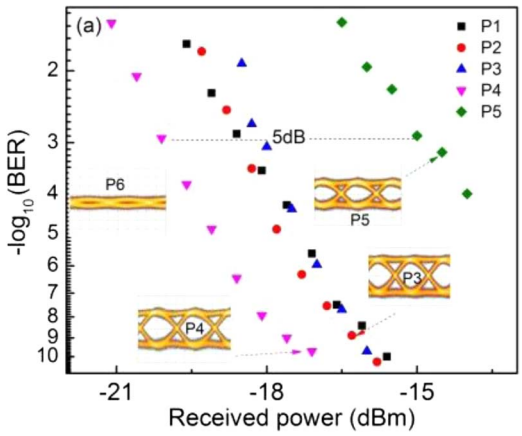

Fig. 7. BER plots versus the received power for the upstream signal in different schemes. (Insets) Eye diagrams for the corresponding schemes.

about 5 dB power penalty was observed for P5 compared to the P4 case. For P6 case, the BER cannot be measured by the BER tester since the upstream data is not modulated onto the optical carrier [21]. Compared to the conventional scheme, P1-P3 cases show nearly identical performance. BER$<10^{-9}$ can all be obtained for P1-P3 cases. This again shows the polarization-independent feature of the proposed scheme.

4. Conclusion

In summary, a bidirectional radio-over-fiber mobile fronthaul architecture with polarization-insensitive RAUs is proposed and studied. Compared with conventional wavelength-reusing scheme, the performance of our proposed scheme is less sensitive to the polarization state of the modulated carriers in the RAU. In our scheme, the polarization tracking devices and alignment processes are not necessary. This highly reduces the complexity and cost of the RAU. Hence it is an attractive candidate for the next-generation integrated fiber wireless access networks. A proof-of-concept experiment is performed to show the feasibility of the proposed scheme. In our results, 1.2 Gb/s QPSK-OFDM DS at 60 GHz band and 5 Gb/s OOK polarization-insensitive US over 15 km SSMF are demonstrated.

Acknowledgment

The authors would like to thank Dr. M. Zhu and Dr. J. Zhang for their valuable advices and fruitful discussions.

References

[1] C. Daniels and R. W. Heath, "60 GHz wireless communications: Emerging requirements and design recommendations," *IEEE Veh. Technol. Mag.*, vol. 2, no. 3, pp. 41–50, Sep. 2007.
[2] S. K. Yong and C.-C. Chong, "An overview of multigigabit wireless through millimeter wave technology: Potentials and technical challenges," *EURASIP J. Wireless Commun. Netw.*, vol. 2007, no. 1, p. 50, Jan. 2007.
[3] R. C. Daniels, J. N. Murdock, T. S. Rappaport, and R. W. Heath, "60 GHz wireless: Up close and personal," *IEEE Microw. Mag.*, vol. 11, no. 7, pp. 44–50, Dec. 2010.
[4] M. Sauer, A. Kobyakov, and J. George, "Radio over fiber for picocellular network architectures," *J. Lightw. Technol.*, vol. 25, no. 11, pp. 3301–3320, Nov. 2007.
[5] Y. Zhang, F. Zhang, and S. Pan, "Optical single sideband polarization modulation for radio-over-fiber system and microwave photonic signal processing," *Photon. Res.*, vol. 2, no. 4, pp. B80–B85, Aug. 2014.
[6] Y. Wang, Y. Xu, X. Li, J. Yu, and N. Chi, "Balanced precoding technique for vector signal generation based on OCS," *IEEE Photon. Technol. Lett.*, vol. 27, no. 23, pp. 2469–2472, Dec. 2015.
[7] K. Xu *et al.*, "Microwave photonics: Radio-over-fiber links, systems, and applications," *Photon. Res.*, vol. 2, no. 4, pp. B54–B63, Aug. 2014.

[8] J. Zheng *et al.*, "Fiber-distributed Ultra-wideband noise radar with steerable power spectrum and colorless base station," *Opt. Exp.*, vol. 22, no. 5, pp. 4896–4907, Mar. 2014.
[9] Y.-T. Hsueh, M.-F. Huang, S.-H. Fan, and G.-K. Chang, "A novel lightwave centralized bidirectional hybrid access network: Seamless integration of RoF with WDM-OFDM-PON," *IEEE Photon. Technol. Lett.*, vol. 23, no. 15, pp. 1085–1087, Aug. 2011.
[10] Z. Jia, J. Yu, and G.-K. Chang, "A full-duplex radio-over-fiber system based on optical carrier suppression and re-use," *IEEE Photon. Technol. Lett.*, vol. 18, no. 16, pp. 1726–1728, Aug. 2006.
[11] B. Wu *et al.*, "Multi-service RoF links with colorless upstream transmission based on orthogonal phase-correlated modulation," *Opt. Exp.*, vol. 23, no. 14, pp. 18323–18329, Jul. 2015.
[12] J. Zheng *et al.*, "Implementation of wavelength reusing upstream service based on distributed intensity conversion in ultrawideband-over-fiber system," *Opt. Lett.*, vol. 38, no. 7, pp. 1167–1169, Apr. 2013.
[13] M. Zhu *et al.*, "Demonstration of 4-band millimeter-wave radio-over-fiber system for multi-service wireless access networks," presented at the Opt. Fiber Commun. Conf., Anaheim, CA, USA, 2013, Paper OM3D.4.
[14] N. Cvijetic, D. Qian, J. Hu, and T. Wang, "44-Gb/s/λ upstream OFDMA-PON transmission with polarization-insensitive source-free ONUs," presented at the Opt. Fiber Commun. Conf., San Diego, CA, USA, 2010, Paper OTuO2.
[15] A. Latif *et al.*, "A performance based comparative analysis of high speed electro absorption and Mach–Zehnder modulators to mitigate chromatic dispersion at 140 GHz millimeter wave," *Adv. Inf. Sci. Serv. Sci.*, vol. 4, no. 20, pp. 368–377, Nov. 2012.
[16] B. Koch, R. Noé, D. Sandel, and V. Mirvoda, "Versatile endless optical polarization controller/tracker/demultiplexer," *Opt. Exp.*, vol. 22, no. 7, pp. 8259–8276, Apr. 2014.
[17] J. Zhang *et al.*, "Transmission of 112 Gb/s PM-RZDQPSK over 960 km with adaptive polarization tracking based on power difference," presented at the 36th Eur. Conf. Exh. Opt. Commun., Torino, Italy, 2010, Paper P2. 09.
[18] B. Koch, R. Noé, V. Mirvoda, and D. Sandel, "1-THz bandwidth of 70-krad/s endless optical polarization control," presented at the Opt. Fiber Commun. Conf., San Francisco, CA, USA, 2014, Paper Th2A.1.
[19] M. Yagi, S. Satomi, and S. Ryu, "Field trial of 160-Gbit/s, polarization-division multiplexed RZ-DQPSK transmission system using automatic polarization control," presented at the Opt. Fiber Commun. Conf., San Diego, CA, USA, 2008, Paper OThT7.
[20] R. Shafik, M. Rahman, and A. Islam, "On the extended relationships among EVM, BER and SNR as performance metrics," *Proc. IEEE ICECE*, 2006, pp. 408–411.
[21] B. Wu *et al.*, "Flexible compensation of dispersion-induced power fading for multi-service RoF links based on a phase-coherent orthogonal lightwave generator," *Opt. Lett.*, vol. 40, no. 9, pp. 2103–2106, May 2015.